Pharmacogenomics and Personalized Medicine

Dovepress

open access to scientific and medical research

Open Access Full Text Article

ORIGINAL RESEARCH

miR-139-5p and miR-451a as a Diagnostic Biomarker in LUSC

Bo Gao[1,*], Rui Li[2,*], Xiaojia Song[3], Shan Hu[4], Fengmei Yang[4]

[1]Departments of Laboratory Medicine, Taihe Hospital, Hubei University of Medicine, Shiyan, Hubei, 442000, People's Republic of China; [2]Departments of Medical office, Taihe Hospital, Hubei University of Medicine, Shiyan, Hubei, 442000, People's Republic of China; [3]Shiyan Prefecture Center for Disease Control and Prevention, Shiyan, Hubei, 442000, People's Republic of China; [4]Departments of Obstetrics and Gynecology, Taihe Hospital, Hubei University of Medicine, Shiyan, Hubei, 442000, People's Republic of China

*These authors contributed equally to this work

Correspondence: Fengmei Yang, Email 29256175@qq.com

Background: Lung squamous cell carcinoma (LUSC) is a type of lung cancer that originates from segmental or subsegmental bronchial mucosa. There is evidence that miRNA plays an important role in the occurrence and progression of tumors.

Methods: In this study, plasma samples of patients with early LUSC and healthy volunteers were subjected to miRNA sequencing, and the levels of differentially expressed miRNAs (DEMs) in LUSC tissues were analyzed using R language. Cox regression and Kaplan–Meier (K-M) survival curve analyses were performed to determine the relationship between DEMs and prognosis in LUSC, and PCR method was verified for the plasma expression level of DEMs in patients with LUSC. The levels of CYFRA21-1 and SCC-Ag in plasma were measured, and area under curve (AUC) was used to evaluate the diagnostic value of the DEMs.

Results: A total of 21 DEMs were screened out by sequencing. The expression levels of DEMs in tissue samples in the TCGA database were analyzed, and four DEMs with consistent expression levels were further screened from plasma and tissue samples. Regression analysis and K-M curve were performed to select two DEMs (miR-139-5p, miR-451a) that were correlated with the prognosis. PCR verification results showed that the levels of miR-451a and miR-139-5p were low in patients, and the level of miR-139-5p in late stages III & IV with the patients of LUSC was higher than that in stages I & II. The AUC values of the four indicators (SCC-Ag, CYFRA21-1, miR-451a and miR-139-5p) in the diagnosis of LUSC, early and late cases were 0.884, 0.935 and 0.778, respectively.

Conclusion: The detection of miR-139-5p and miR-451a levels in plasma has a certain potential in the non-invasive diagnosis, especially in patients with early stages of LUSC.

Keywords: miR-139-5p, LUSC, miR-451a, diagnosis, prognosis

Introduction

Lung cancer is the most common primary lung malignant tumor and is a malignant tumor originating from respiratory epithelial cells. Squamous cell carcinoma is a relatively common subtype, and approximately 75% of patients diagnosed are already in the late stages of the disease.[1,2] In LUSC, the prevention and treatment strategy of "early detection, early diagnosis and early treatment" can effectively reduce morbidity.[3] For early detection, the sensitivity and specificity of serum markers, such as squamous cell carcinoma antigen (SCC-Ag) and Cytokeratin-19-fragment (CYFRA21-1), are low, and cannot meet clinical needs.[4] Therefore, finding novel tumor markers with high sensitivity and specificity is important to diagnose tumors.

miRNAs are small non-coding RNAs and play an important role in regulating the occurrence of disease.[5] They can also regulate cell apoptosis, development, proliferation and differentiation, and can serve as tumor suppressor genes or oncogenes,[6,7] which can be used as potential indicators for tumor diagnosis.[8] Therefore, measuring the expression levels of miRNAs in the plasma of tumor cases is helpful to discover the miRNAs associated with tumorigenesis and elucidate the underlying mechanisms.[9,10] In this study, high-throughput miRNA sequencing was used to compare

Received: 3 February 2023
Accepted: 31 March 2023
Published: 8 April 2023

DEMs in plasma between tumor patients and healthy volunteers and to screen out DEMs, laying a foundation for subsequent research.

Materials and Methods

Clinical Sample Collection

Samples of EDTA anticoagulant peripheral blood (10mL) were collected from three patients with early LUSC (StageI 2, StageII 1) and three healthy volunteers, and plasma was separated at 4°C and stored in liquid nitrogen for miRNA sequencing. Peripheral blood specimens from 42 cases with LUSC and 20 healthy people were collected, and the plasma was separated at 4°C and stored in liquid nitrogen for PCR and determination of tumor markers. None of the patients underwent preoperative radiotherapy or chemotherapy. In accordance with the Declaration of Helsinki, all protocols were approved by the Ethics Committee of Taihe Hospital. Either informed consent was obtained for the cases or, if they were unable to provide informed consent because of diminished capacity or language barrier or memory impairment, from designated health-care surrogates. All informed consents or surrogate consents were approved by the Ethics Committee of Taihe Hospital and were documented accordingly.

miRNA Sequencing

The sequencing steps include: RNA extraction, detection of RNA distribution, construction library of small RNA sample, the detection of concentration and quality, detection of insertion size of the library, library sequencing by Hiseq/Miseq and pooling different libraries according to effective concentration. The sequencing reagents include RNEasy Mini Kit and Small RNA Sample Pre Kit. The sequencing Instruments include Agilent 2100 PIC600, Agilent 2100 and ABI7500.

Quality Control of Sequencing Data

To ensure the quality of information analysis, raw data from NGS (Next-Generation Sequencing, NGS) were converted into raw reads by base calling and must be processed to obtain clean reads, which often contained low-quality reads with connectors. Base calling is an algorithm (software) that identifies the base type (DNA sequence) from the raw images (original image), writes the results into a cal file, and finally helps us to generate the sequencing report and FastQ data. Steps for processing raw reads to clean reads include removing reads containing an adapter or ploy-N, and low-quality reads with connectors or from raw data. Clean reads of each sample were screened, and sRNA analysis was performed within a certain length range. A threshold value of $|\log2\text{Fold Change}|>1$ and $P<0.05$ was determined.

DEMs and K-M Survival Analysis in Tissue Samples

The expression of DEMs in tissue samples and their effect on the prognosis and survival of patients with LUSC were determined. The tool "Starbase" was used to analyze DEMs and K-M survival in tissue samples. The miRNA sequencing data of LUSC were downloaded from TCGA (https://portal.gdc.cancer.gov/), and K-M was analyzed using R language, and the PROGNOSIS and survival curves of DEMs. Meanwhile, a Cox regression model of miRNA expression was constructed to analyze the prognostic value of DEMs level in LUSC.

RT-qPCR Analysis

Qiagen RNEasy Mini Kit (Qiagen, Germany) was used to extract the RNA, and RT-qPCR was used to analyze DEMs in peripheral plasma samples from 42 LUSC patients and 20 healthy volunteers. After reverse transcription, PCR system was prepared using SYBRGreen kit (Qiagen, Germany), and amplification was performed using ABI7500 (Thermo Fisher, USA). The correlation between DEMs and clinical features was evaluated. DEMs were also normalized to U6 and were determined using the $2^{-\Delta\Delta Ct}$ method.

The Detection of Plasma Markers

The level of tumor markers CYFRA21-1, SCC-Ag were detected using a Roche Cobas 601 chemiluminescence equipment (Roche, Switzerland). Reagents were used to support the instrument. All reagents were standardized before detection. The detection results of CYFRA21-1>3.3ng/mL and SCC-Ag>1.5ng/mL indicated increased tumor marker levels.

Statistical Analysis

Statistical analysis was performed using SPSS software version 16.0 (SPSS Inc. Chicago, IL). The measured data were expressed as the mean±standard deviation and Kaplan–Meier method was used for survival analysis. The value of DEMs in the diagnosis of LUSC was analyzed by Receiver Operating Characteristic curve (ROC). $P<0.05$ was used to indicate a statistically significant difference.

Result

Overview of the miRNA Sequencing Results

Raw data from NGS were converted into raw reads by base calling, and the quality of raw data produced by sequencing all samples is shown in Supplementary Table 1. sRNA of all tumor and normal samples were compared to screen out known and novel miRNAs (Table 1). Meanwhile, the levels of DEMs in every plasma were counted, and the DEM levels were normalized with Transcripts Per Million (TPM). The TPM density distribution of different samples is shown in Figure 1A, and the correlation of gene expression levels is shown in Figure 1B. DEMs were screened from identified miRNAs by comparing with miRNA localization sequences. According to these criteria, 21 DEMs were collected in tumor and normal samples (Table 2). The data were 12 up-regulated and 9 down-regulated in these DEMs and were shown by volcanic map (Figure 1C) and cluster analyses (Figure 1D).

Expression Level of DEMs in Tumor Tissue

DEMs in plasma were screened by high-throughput sequencing, and these miRNAs were compared within "starBase" and TCGA database to verify the DEMs levels in tissue and plasma. Four DEMs (miR-451a, miR-139-5p, miR-200a-3p and miR-205-5p) levels in tissue were consistent with plasma expression levels (Figure 2A–D). The expression levels of these DEMs were consistent with those in "starbase" and plasma by unpaired and paired samples analysis (Figure 2E–F).

The Prognostic Value of miRNA Expression Level by Regression Analysis

Sequencing data of miRNA were downloaded in the TCGA database. A prognostic Cox regression model of miRNA expression was constructed, and the expression level DEMs (12 up-regulated and 9 down-regulated) associated with the prognosis of LUSC were analyzed (Supplementary Table 2). Univariate regression analysis showed that the expression level of miR-139-5p was the prognostic factor (Figure 3A), and multivariate regression analysis showed that the expression levels of miR-451a and miR-139-5p were the prognostic factors (Figure 3B). The above studies indicated that the expression levels of these DEMs in tumor tissues by "starBase" and TCGA database were consistent with those in plasma by miRNA sequencing. Regression analysis revealed that low expression levels of miR-139-5p and miR-451a in plasma were the prognostic factors in patients with LUSC.

Table 1 Matching miRNA in All Sample

Types	N1	N2	N3	T1	T2	T3
Total	2,426,982	3,800,077	3,946,393	2,224,822	2,359,407	2,220,667
Known_miRNA	431292	783,071	1,096,545	222,025	267,331	571,944
Novel_miRNA	90	62	94	51	53	93

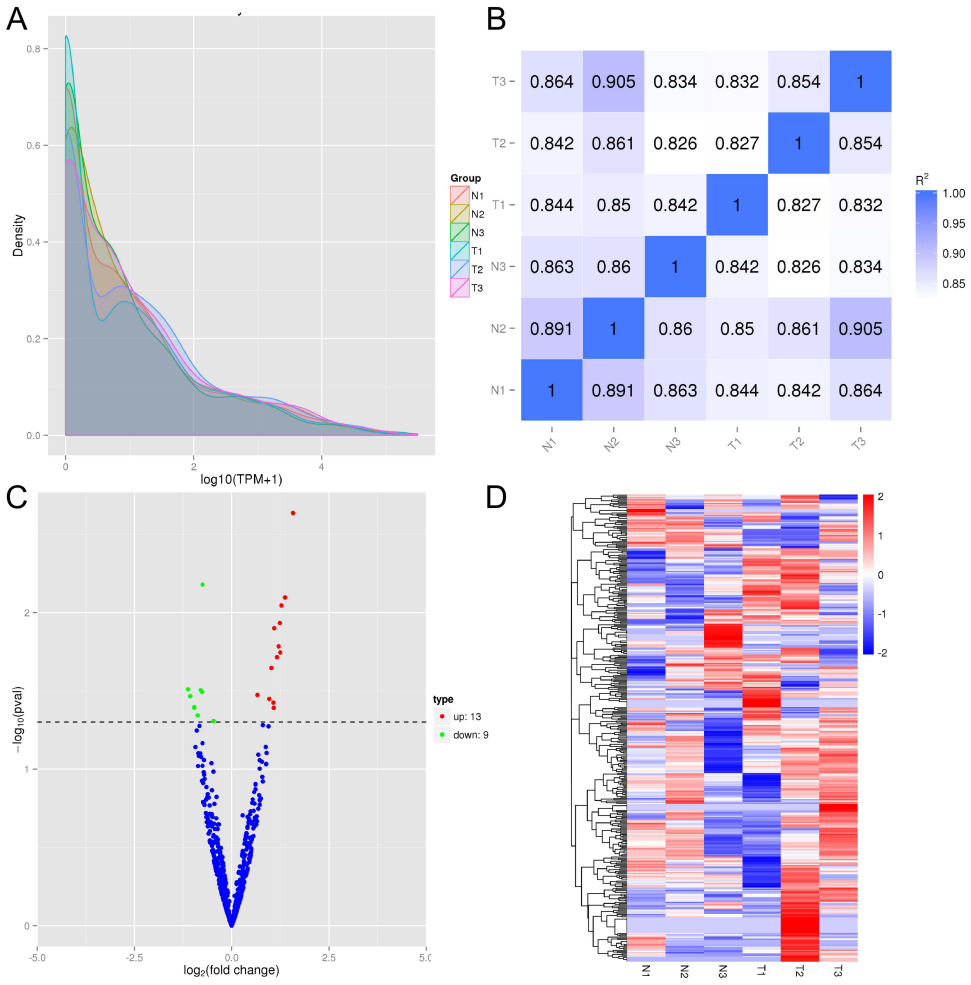

Figure 1 Overview of the miRNA Sequencing Results. (**A**) TPM density distribution in all samples. The distribution of TPM density could be used to examine the gene expression pattern of the sample. The x-coordinate was the log10 (TPM+1) value of miRNA, and the y-coordinate was the density of the corresponding log10 (TPM+1); (**B**) Pearson correlation between samples. The correlation of gene expression level between samples was an important index to test the reliability of the experiment and the rationality of the sample selection. The closer the correlation coefficient was to 1, the higher the similarity of expression patterns between samples. (**C**) Volcano plot of the differential expression profiles of miRNAs. Blue dots represent miRNAs with no significant difference, red dots represent significantly up-regulated differential miRNAs, and green dots represent significantly down-regulated differential miRNAs; (**D**) Heatmap of the differential expression profiles of miRNAs. Red represents high expression miRNAs, blue represents low expression miRNAs.
Note: Abbreviations: "N", Normal sample; "T", Tumor sample.

The Relationship Between DEMs Levels and Survival Time

In this study, the correlation was analyzed between DEMs levels and overall survival (OS) in the StarBase database. A low level of miR-451a had a shorter OS (Figure 4A), whereas a high level of miR-139-5p had a shorter OS in patients with LUSC (Figure 4C). In addition, miRNA sequencing data of LUSC were downloaded for K-M analysis from the

Table 2 Differentially Expressed miRNAs in the Plasma of Tumor Group and Healthy Group

Symbol	T_readcount	N_readcount	log FC	P value
Up regulation				
hsa-miR-375	634.7353697	97.41763536	1.5777	0.0023146
hsa-miR-215-5p	1207.757101	328.296555	1.2809	0.0089933
hsa-miR-200a-3p	221.4756267	83.67566833	1.0918	0.012566
hsa-miR-378a-5p	12.30129588	3.236560489	1.2066	0.016426
hsa-miR-1306-5p	6.988734754	1.024093283	1.2485	0.01796

(*Continued*)

Table 2 (Continued).

Symbol	T_readcount	N_readcount	log FC	P value
hsa-miR-205-5p	22.43066366	6.812933893	1.1616	0.01922
hsa-miR-29b-3p	40.61579593	16.25698968	1.0196	0.022594
hsa-miR-411-5p	63.31949599	38.23398694	0.6651	0.033586
hsa-miR-296-3p	9.752932951	2.623827248	1.0729	0.037562
hsa-miR-136-3p	18.16702912	3.431958038	1.0796	0.040537
novel_320	3.70336313	0	1.2373	0.011644
novel_352	16.49353068	3.033868294	1.3735	0.0080016
novel_384	4.167335423	0	0.96574	0.035588
Down regulation				
hsa-miR-182-5p	269.1106763	474.078997	−0.7499	0.0066161
hsa-miR-379-3p	0.445869148	5.509323188	−1.1218	0.030872
hsa-miR-139-5p	899.8418231	1712.624201	−0.7961	0.031279
hsa-miR-451a	91,101.09974	167,131.6751	−0.7613	0.032178
hsa-miR-589-5p	4.45992082	13.84252783	−1.0657	0.034194
hsa-miR-3158-3p	82.86516964	206.4113518	−0.9649	0.040149
hsa-miR-3158-5p	82.86516964	205.7813913	−0.9627	0.040442
hsa-miR-15a-5p	10.71164688	23.87013827	−0.8772	0.045288
hsa-miR-25-3p	3659.071768	5146.814994	−0.4662	0.049296

TCGA database. K-M survival curve also showed similar results (Figure 4B and D). In addition, in stages of T1&T2, N0, M0 and StageI&StageII, a low expression of miR-451a had a shorter OS (Figure 5A–D), and a high expression of miR-139-5p had a shorter OS in patients with LUSC (Figure 5E–H).

The Expression of DEMs in Validation Samples

The relative expression levels of miR-451a and miR-139-5p in the plasma of 42 patients with LUSC and 20 normal people were detected. The expression levels of miR-451a and miR-139-5p in plasma of LUSC were significantly lower than in those of healthy controls are shown in Figure 6. Comparison of miRNAs levels in patients with different clinical subtypes showed that the expression levels of miR-139-5p in stage III and IV were higher than those in stage I and II. No significant differences in the levels of miR-451a and miR-139-5p were founded in other clinicopathological characteristics (gender, age, smoking history, stage, and lymph node metastasis) (Supplementary Table 4).

Diagnostic Analysis of DEMs in LUSC

In patients with LUSC, we detected the plasma levels of SCC-Ag, CYFRA21-1, miR-451a, miR-139-5p, and researched the values of miR-451a, miR-139-5p as indicators in the diagnosis of LUSC and early patients (StageI&II). The expression levels of miR-451a and miR-139-5p were downloaded to predict the diagnostic efficacy of miRNAs from TCGA. In Figure 7A, the AUC of miR-451A for the diagnosis of LUSC was 0.931, with a specificity of 82.6% and a sensitivity of 91.1%, whereas the AUC of miR-139-5p for the diagnosis of LUSC was 0.960, with a specificity of 92.3% and a sensitivity of 97.8%. In this study, the AUC, specificity and sensitivity of four indicators (miR-139-5p, miR-451a, CYFRA21-1 and SCC-Ag) in the diagnosis of lung squamous cell carcinoma, early patients and late patients are shown in Figure 7B-7D and Supplementary Table 3.

Discussion

As a major subtype of non-small cell lung cancer (NSCLC), lung squamous cell carcinoma occurs proximal to the lung and originates primarily from bronchial basal cells.[11] Unlike lung adenocarcinoma, patients with lung squamous cell carcinoma (LSCC) have not benefited from targeted therapies.[12] Diagnosis is often challenging, particularly in small biopsy specimens. Thus, treatment options are limited. In contrast to lung adenocarcinoma, targeted therapy for LUSC

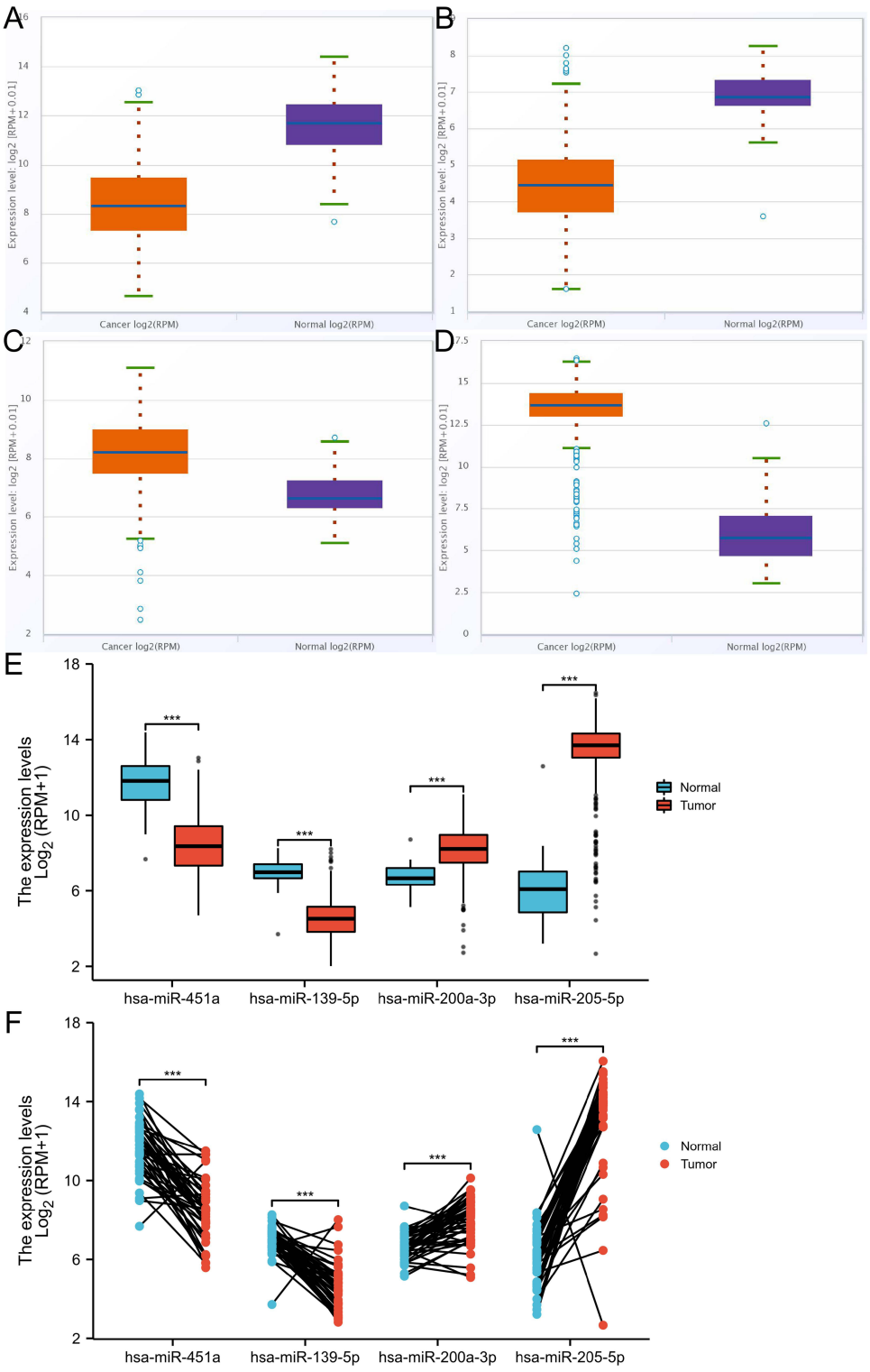

Figure 2 The expression of DEMs in tumor tissues using "starbase" and TCGA. (**A**–**D**) was "starbase" tool, (**E** and **F**) was TCGA. (**A**) the expression of hsa-miR-451a; (**B**) The expression of hsa-miR-139-5p; (**C**) The expression of hsa-miR-200a-3p; (**D**) The expression of hsa-miR-205-5p; (**E**) The expression of DEMs in paired samples; (**F**) The expression of DEMs in unpaired samples.***P<0.001.

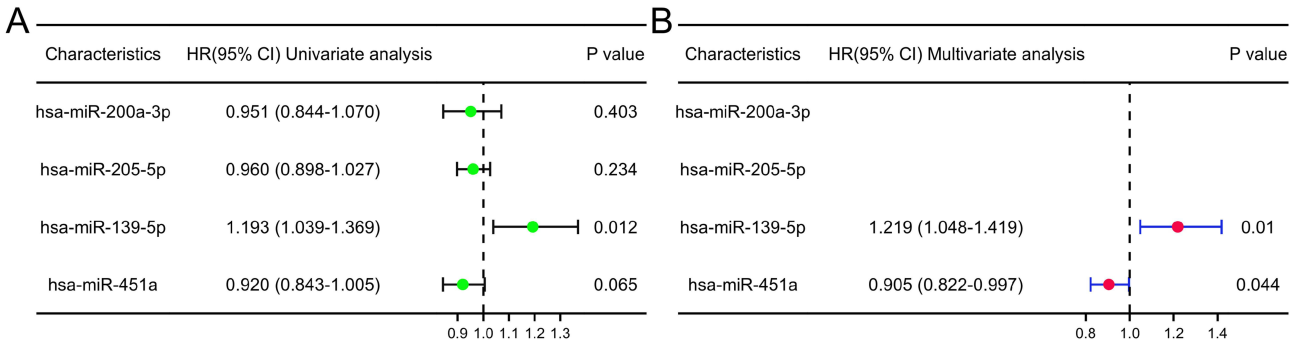

Figure 3 Forest plot of Cox multivariate analysis of for miRNAs (hsa-miR-451a, hsa-miR-139-5p, hsa-miR-200a-3p and hsa-miR-205-5p). (**A**) Univariate analysis; (**B**) Multivariate analysis.

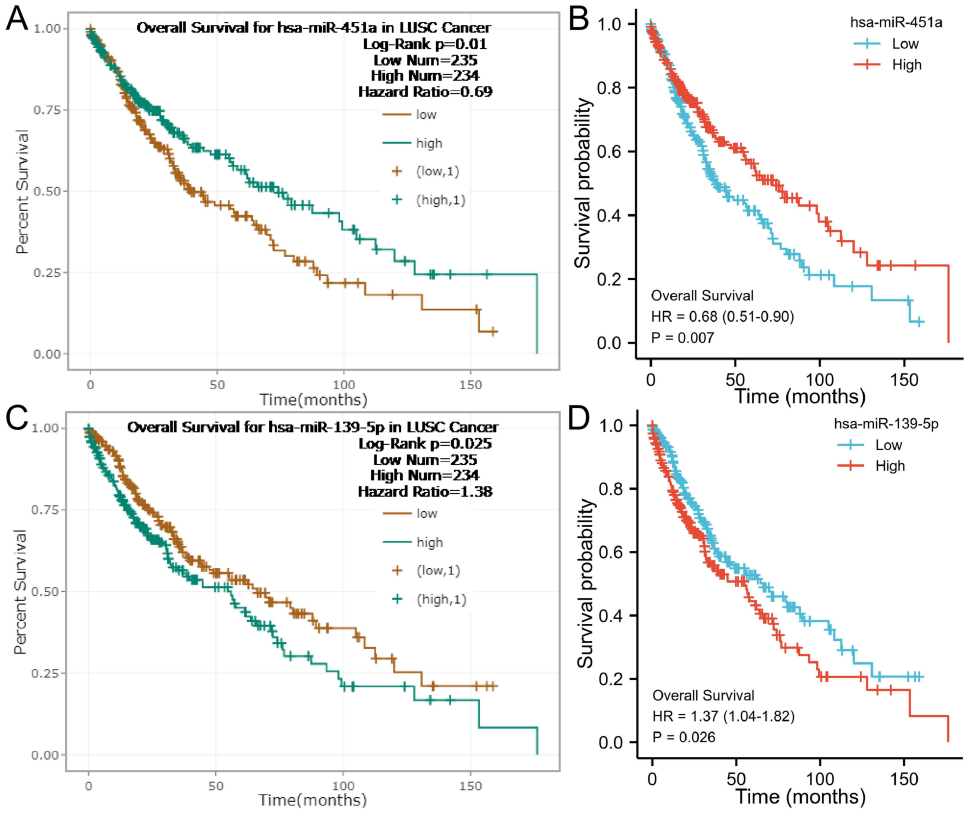

Figure 4 The relationship between miRNAs expression and OS using "starbase" and K-M. (**A** and **C**) Survival analysis using "starbase" tool; (**B** and **D**) Survival analysis using K-M.

remains unsuccessful.[13] Therefore, it is particularly important to find novel markers for the early diagnosis of LUSC using high-throughput sequencing or other methods.

In this study, the expression of DEMs in LUSC was analyzed by high-throughput sequencing, "starBase", TCGA database, and PCR validation. Results showed that miR-139-5p and miR-451a were down-regulated in the plasma and tissues with patients of LUSC. Furthermore, their expression levels were correlated with the prognosis of patients with LUSC.

Compared with the wild type of Kras gene, miR-139-5p expression is significantly down-regulated in colorectal cancer cells and tissues with Kras mutation. The expression of miR-139-5p is down-regulated in different tumors and plays an important role in tumorigenesis. Low expression of miR-139-5p has been correlated with an aggressive phenotype and poor prognosis in colorectal cancer patients.[14] In vivo, overexpression of miR-139-5p can make tumors

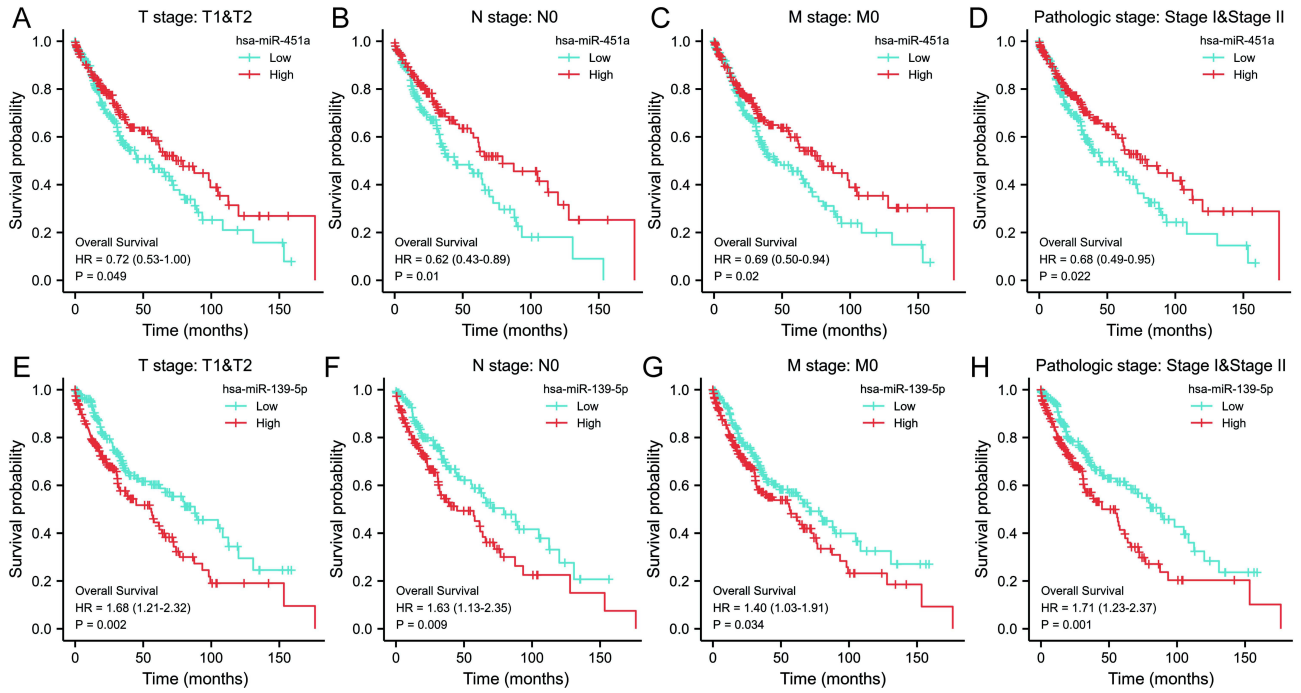

Figure 5 The relationship between miRNAs expression and OS in clinical subtypes. (**A**–**D**) was hsa-miR-451a, (**E**–**H**) was hsa-miR-139-5p.

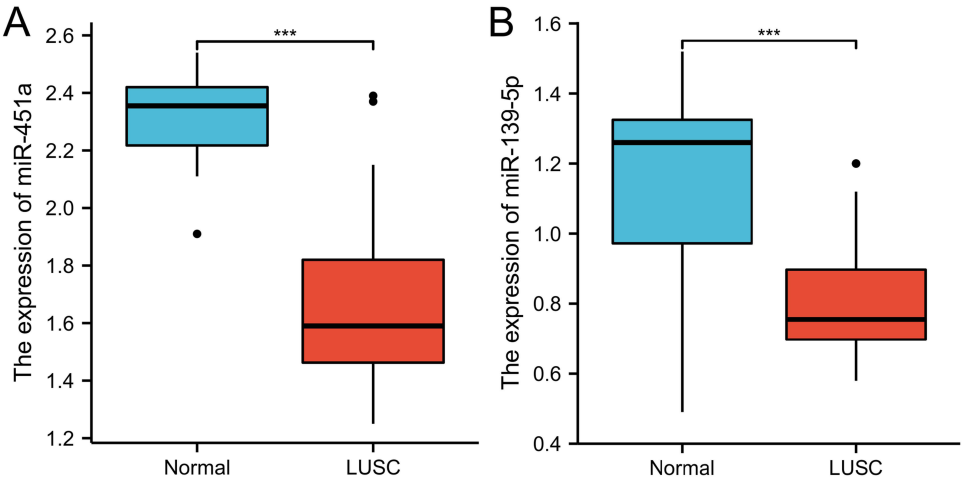

Figure 6 The expression of hsa-miR-451a and hsa-miR-139-5p in the plasma of LUSC and health people. (**A**) hsa-miR-451a; (**B**) hsa-miR-139-5p. ***P<0.001.

sensitive to chemotherapy and inhibit tumor growth and metastasis, and in colorectal cancer cells, overexpression of miR-139-5p can inhibit proliferation, migration and invasion.[15] Similarly, in hepatocellular carcinoma (HCC) cells, miR-139-5p expression is down-regulated in HCC, and miR-139-5p overexpressed can inhibit proliferation, migration and invasion.[16]

DEMs exert different effects as prognostic indicators in different tumors. Interestingly, low level of miR-451a and miR-139-5p in LUSC shows a different relationship with prognosis. In the present study, K-M analysis showed that a high level of miR-139-5p had a lower OS, whereas those with a high expression of miR-451a had a higher OS in patients with LUSC. This result was also true in early patients. Downregulation of miR-451a was confirmed in LUSC clinical specimens, and low expression of miR-451a was found to be significantly associated with poor prognosis in patients with LUSC.[17] Furthermore, downregulation of miR-451 was detected in NSCLC tissues and its expression was

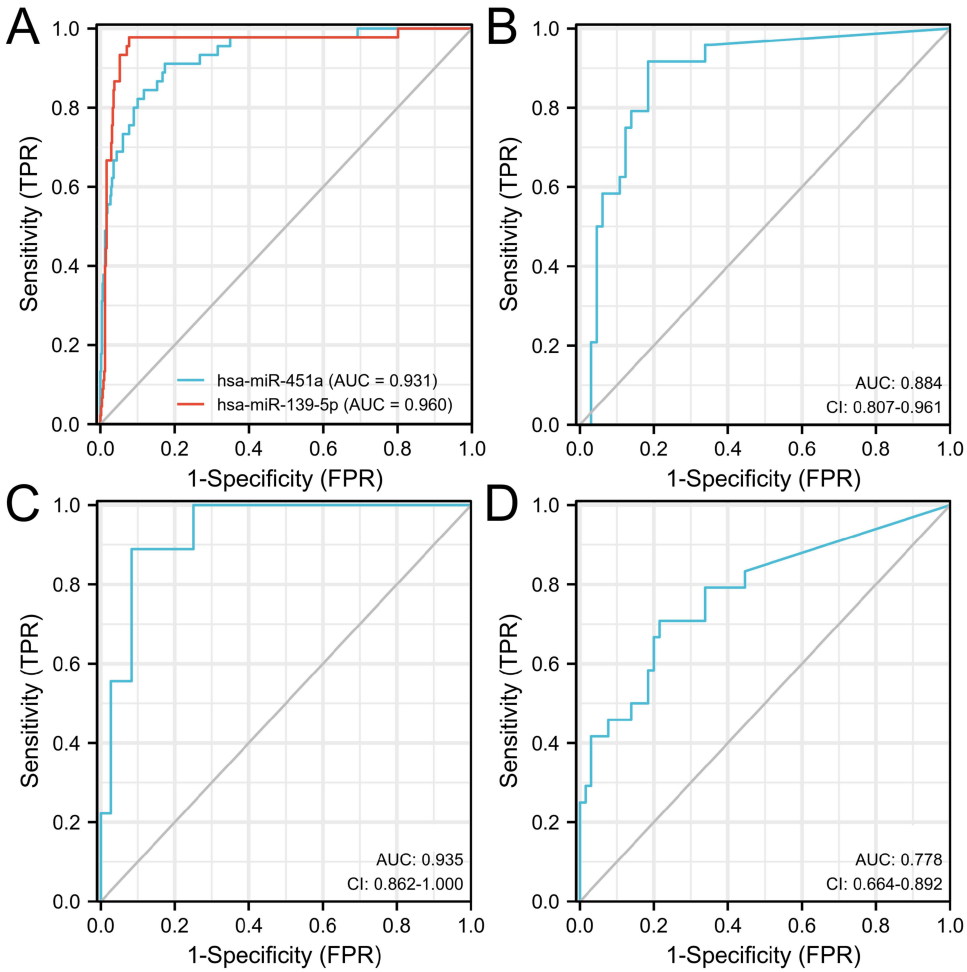

Figure 7 ROC curve analysis of miRNA expression level in the diagnosis of LUSC. (**A**) ROC curve of hsa-miR-451a and hsa-miR-139-5p expression in diagnosis of LUSC by bioinformatics analysis; (**B**) ROC curve of four indicators for diagnosis of LUSC; (**C**) ROC curve of four indicators for diagnosis of Stage I&II; (**D**) ROC curve of four indicators for diagnosis of Stage III&IV.

an independent predictor of prognosis of NSCLC, such as advanced disease stage and metastasis. Interestingly, ectopic expression of miR-451 suppressed cell proliferation, migration, and activation of AKT through targeting MIF in NSCLC cells.[18] Moreover, prostate cancer patients with high miR-451a expression in the blood have significantly lower OS than those with low expression.[19] In prostate cancer patients, the expression of miR-451a is down-regulated, and patients with a high expression level of miR-451a have a worse prognosis.[20] In myeloma, miR-451a can regulate the apoptosis and proliferation of cells and can be used to predict the prognosis, and this mechanism may be related to the regulation of the IL-6R/JAK2/STAT3 pathway.[21] In peripheral blood of patients with multiple myeloma, circulating miR-451a levels may be a novel biomarker and play a role in monitoring minimal residual disease and predicting recurrence in patients.[22]

In adrenocortical carcinoma, a higher level of miR-139-5p has been associated with worse OS compared with a low miR-139-5p level. In patients with HCC, miR-139-5p is also a prognostic indicator, and its expression is negatively correlated with OS and relapse-free survival (RFS).[23] Mechanistically, miR-139-5p might negatively regulate CCNB1 in LUAD, thereby suppressing cell proliferation, migration, invasion and cell cycle.[24] However, esophageal cancer patients with low miR-139-5p expression have significantly lower survival rates than those with high expression,[25] and gallbladder cancer patients with low miR-139-5p expression level were more likely to have a lower OS rate.[26] This result may be caused by the different signaling pathways involved in miR-139-5p in different tumors. For example, the Wnt/β-catenin, PI3K/AKT/mTORC1 and RTK/RAS/MAPK pathways. These most important signaling pathways of miR-

139-5p are common in other miRNAs related to cancer suppression or progression and involve in tumorigenesis,[27] and the role of the miR-139-5p/Notch1 axis in glioma prognosis has been confirmed.[28]

In the presented study, we found that miR-451a and miR-139-5p are good biomarkers for the diagnosis of LUSC, especially in patients in the early stages of the disease. Thus, these biomarkers may improve the diagnostic accuracy, especially when combined with other available biomarkers (CYFRA21-1, SCC-Ag). We also analyzed whether miR-139-5p and miR-451a in early patients have similar diagnostic values in late patients. We found that the early model had weak diagnostic ability for patients with late patients,[29] indicating that early markers can be roughly presented in each stage of LUSC. However, this result confirms that early-stage markers can generally present the molecular characteristics of LUSC in all stages.

Conclusion

In conclusion, in the peripheral plasma of patients with LUSC, the low level of miR-451a and miR-139-5p can be used as a good indicator for the diagnosis of LUSC, especially in patients with early disease.

Disclosure

The authors report no conflicts of interest in this work.

References

1. Nooreldeen R, Bach H. Current and future development in lung cancer diagnosis. *Int J Mol Sci*. 2021;22:16. doi:10.3390/ijms22168661
2. Wan L, Cheng Z, Sun Q, et al. LncRNA HOXC-AS3 increases non-small cell lung cancer cell migration and invasion by sponging premature miR-96. *Expert Rev Respir Med*. 2022;16(5):587–593. doi:10.1080/17476348.2022.2030223
3. Wu F, Wang L, Zhou C. Lung cancer in China: current and prospect. *Curr Opin Oncol*. 2021;33(1):40–46. doi:10.1097/CCO.0000000000000703
4. Zhao Y, Liu Y, Li S, et al. Role of lung and gut microbiota on lung cancer pathogenesis. *J Cancer Res Clin Oncol*. 2021;147(8):2177–2186. doi:10.1007/s00432-021-03644-0
5. Imyanitov EN, Iyevleva AG, Levchenko EV. Molecular testing and targeted therapy for non-small cell lung cancer: current status and perspectives. *Crit Rev Oncol Hematol*. 2021;157:103194. doi:10.1016/j.critrevonc.2020.103194
6. Flemming JP, Hill BL, Haque MW, et al. miRNA- and cytokine-associated extracellular vesicles mediate squamous cell carcinomas. *J Extracell Vesicles*. 2020;9(1):1790159. doi:10.1080/20013078.2020.1790159
7. He R, Feng X, Yang K, et al. Construction of a 5-methylcytosine-related molecular signature to inform the prognosis and immunotherapy of lung squamous cell carcinoma. *Expert Rev Mol Diagn*. 2022;22(9):905–913. doi:10.1080/14737159.2022.2131396
8. Hill M, Tran N. miRNA interplay: mechanisms and consequences in cancer. *Dis Model Mech*. 2021;14:4. doi:10.1242/dmm.047662
9. Pawlick JS, Zuzic M, Pasquini G, et al. MiRNA regulatory functions in photoreceptors. *Front Cell Dev Biol*. 2020;8:620249. doi:10.3389/fcell.2020.620249
10. Kujtan L, Kancha RK, Gustafson B, et al. Squamous cell carcinoma of the lung: improving the detection and management of immune-related adverse events. *Expert Rev Anticancer Ther*. 2022;22(2):203–213. doi:10.1080/14737140.2022.2029414
11. Gomez-Lopez S, Whiteman ZE, Janes SM. Mapping lung squamous cell carcinoma pathogenesis through in vitro and in vivo models. *Commun Biol*. 2021;4(1):937. doi:10.1038/s42003-021-02470-x
12. Niu Z, Jin R, Zhang Y, et al. Signaling pathways and targeted therapies in lung squamous cell carcinoma: mechanisms and clinical trials. *Signal Transduct Target Ther*. 2022;7(1):353. doi:10.1038/s41392-022-01200-x
13. Pan Y, Han H, Labbe KE, et al. Recent advances in preclinical models for lung squamous cell carcinoma. *Oncogene*. 2021;40(16):2817–2829. doi:10.1038/s41388-021-01723-7
14. Du F, Cao T, Xie H, et al. KRAS mutation-responsive miR-139-5p inhibits colorectal cancer progression and is repressed by wnt signaling. *Theranostics*. 2020;10(16):7335–7350. doi:10.7150/thno.45971
15. Miyoshi J, Toden S, Yoshida K, et al. MiR-139-5p as a novel serum biomarker for recurrence and metastasis in colorectal cancer. *Sci Rep*. 2017;7:43393. doi:10.1038/srep43393
16. Wu J, Zhang T, Chen Y, et al. MiR-139-5p influences hepatocellular carcinoma cell invasion and proliferation capacities via decreasing SLITRK4 expression. *Biosci Rep*. 2020;40(5). doi:10.1042/BSR20193295
17. Uchida A, Seki N, Mizuno K, et al. Regulation of KIF2A by antitumor miR-451a inhibits cancer cell aggressiveness features in lung squamous cell carcinoma. *Cancers*. 2019;11:2. doi:10.3390/cancers11020258
18. Editors PO. Expression of Concern: the low expression of miR-451 predicts a worse prognosis in non-small cell lung cancer cases. *PLoS One*. 2023;18(1):e0280774.
19. Fan B, Jin X, Ding Q, et al. Expression of miR-451a in prostate cancer and its effect on prognosis. *Iran J Public Health*. 2021;50(4):772–779. doi:10.18502/ijph.v50i4.6002
20. Zhao F, Wei C, Cui MY, et al. Prognostic value of microRNAs in pancreatic cancer: a meta-analysis. *Aging*. 2020;12(10):9380–9404. doi:10.18632/aging.103214
21. Zhong L, Xu Z, Jin X, et al. miR-451a suppression of IL-6R can inhibit proliferation and increase apoptosis through the JAK2/STAT3 pathway in multiple myeloma. *Oncol Lett*. 2020;20(6):339. doi:10.3892/ol.2020.12202
22. Zhong L, Jin X, Xu Z, et al. Circulating miR-451a levels as a potential biomarker to predict the prognosis of patients with multiple myeloma. *Oncol Lett*. 2020;20(5):263. doi:10.3892/ol.2020.12126

23. Wang X, Gao J, Zhou B, et al. Identification of prognostic markers for hepatocellular carcinoma based on miRNA expression profiles. *Life Sci*. 2019;232:116596. doi:10.1016/j.lfs.2019.116596
24. Bao B, Yu X, Zheng W. MiR-139-5p Targeting CCNB1 modulates proliferation, migration, invasion and cell cycle in lung adenocarcinoma. *Mol Biotechnol*. 2022;64(8):852–860. doi:10.1007/s12033-022-00465-5
25. Jiao W, Zhang J, Wei Y, et al. MiR-139-5p regulates VEGFR and downstream signaling pathways to inhibit the development of esophageal cancer. *Dig Liver Dis*. 2019;51(1):149–156. doi:10.1016/j.dld.2018.07.017
26. Chen J, Yu Y, Chen X, et al. MiR-139-5p is associated with poor prognosis and regulates glycolysis by repressing PKM2 in gallbladder carcinoma. *Cell Prolif*. 2018;51(6):e12510. doi:10.1111/cpr.12510
27. Niveditha D, Jasoria M, Narayan J, et al. Common and unique microRNAs in multiple carcinomas regulate similar network of pathways to mediate cancer progression. *Sci Rep*. 2020;10(1):2331. doi:10.1038/s41598-020-59142-9
28. Li J, Li Q, Lin L, et al. Targeting the Notch1 oncogene by miR-139-5p inhibits glioma metastasis and epithelial-mesenchymal transition (EMT). *BMC Neurol*. 2018;18(1):133. doi:10.1186/s12883-018-1139-8
29. Lu H, Liu Y, Wang J, et al. Detection of ovarian cancer using plasma cell-free DNA methylomes. *Clin Epigenetics*. 2022;14(1):74. doi:10.1186/s13148-022-01285-9